

PRESSURE MEASUREMENTS WITHIN A LARGE TORNADO

Timothy M. Samaras *

Julian J. Lee*

Applied Research Associates, Inc.

1. ABSTRACT

Making accurate barometric pressure measurements in tornado cores is difficult due to very high wind velocities, heavy rain, and wind-driven debris. For a pressure probe to remain stationary during a tornado passage, special considerations must be applied to the physical geometry of the device. The actual barometric or free-stream static pressure measurement with a probe represents a special challenge as the curvature of the streamlines over any object will alter the measurement. This is especially important in wind velocities exceeding 80 meters/second, as has been measured and predicted in tornado cores. A specially-designed hardened probe called a "Hardened In-Situ Tornado Pressure Recorder (HITPR) has been developed by the author at Applied Research Associates Inc. The HITPR has met all of the challenges discussed above, and as a result of detailed aerodynamic characterization, wind speed and wind direction are also measured, along with the air temperature and relative humidity. The measurement technique will be described as well as actual pressure measurements from a successful tornado interception in Pratt, Kansas on May 7th, 2002.

2. INTRODUCTION

A new tool has been developed at Applied Research Associates Inc. (ARA) for In-Situ measurements in tornado cores. The Hardened In-Situ Tornado Pressure Recorder (HITPR) is a self-contained hardened instrument with no moving parts that records pressure, temperature, relative humidity, wind speed, and wind direction within a tornado core. Thanks to its unique conical shape, the HITPR accurately records the

static pressure in the presence of high winds. The HITPR was designed to be placed on the ground directly in the path of tornado cores and recovered after tornado passage by chase/research teams. The data is then downloaded and reviewed within minutes of recovery. The HITPR operation is simple, one switch puts the HITPR in record mode, thus deployment can be accomplish in less than 10 seconds which is critical to the chase team.

This paper discusses the design of the probe along with results from a successful deployment near Pratt, Kansas, on May 7th, 2002.

3. PROBE DESIGN CRITERIA

The HITPR probe was designed to accurately measure the static pressure in winds of 40 meters/second or higher. The probe was also designed to survive the harsh environments within a tornado core. It also records the temperature and humidity along with wind speed and wind direction. Hence the original design criterion of measuring static pressure was met and exceeded in the current design of the HITPR probe.

The outer shell is conically shaped (Fig. 1) and is constructed of 6-millimeter thick mild steel. Once the probe is activated, the internal data logger records over 18 channels of information for a duration of two hours. After two hours, the probe goes into a power-saving mode until it is recovered after tornado passage. There is sufficient on-board memory to deploy the HITPR four times in succession without having to download any data.

* Corresponding author address: Timothy M. Samaras, Applied Research Associates, Inc. , Littleton, CO 80127; e-mail: tsamaras@ara.com
Julian J. Lee, Applied Research Associates, Inc. , Littleton, CO 80127; e-mail: jlee@ara.com.



Fig. 1 Picture of HITPR Probe.

4. PRINCIPLE OF OPERATION

The HITPR measures the free-stream static pressure by taking advantage of its aerodynamically profiled body. The variation of the pressure was measured over the entire body of the HITPR over a range of wind speeds from 24 m/s to 101 m/s. These measurements were performed in a wind tunnel. The pressure coefficient (C_p) was then calculated using the expression (Eq. 1):

$$C_p = \frac{P_m - P_s}{\frac{1}{2} \rho V^2}$$

P_m = measured pressure
 P_s = static pressure
 ρ = air density
 V = wind speed

Eq. 1. Relation for the pressure coefficient.

The variation of C_p along the wind axis through the center of the HITPR body was found as a function of the non-dimensionalized distance from the front of the body (X/L) as shown in Fig. 2. The pressure on the body surface was measured for different radii (r) and azimuthal angle (θ). When C_p is zero, the pressure at the surface is equal to the free-stream static pressure (Eq. 1). Measuring the pressure at the point where $C_p = 0$ thus provides a measurement of the static pressure.

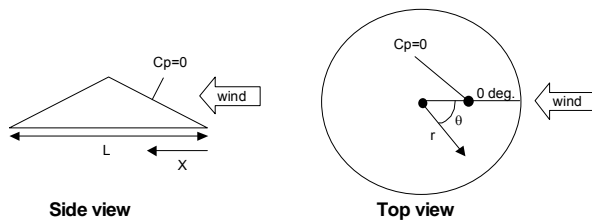


Fig. 2. Schematic diagram of the HITPR.

1.1 Position Of The $C_p=0$ Location

The exact location where $C_p=0$ was determined from the C_p measurements over the entire HITPR body. The variation of C_p in the wind axis along front of the body (for X/L from zero to 0.5) is shown in Fig. 3. C_p decreased steadily from about 0.7 as we progress from the front of the body towards the rear. The $C_p=0$ location was found at $X/L \approx 0.30$. C_p continues to decrease as we progress further towards the rear of the body. For wind speeds of 45 m/s and above, C_p was found to be independent of the wind speed. At 24 m/s, the C_p dependence on X/L was found to be slightly shifted due to Reynolds number effects such as transition between laminar and turbulent flow and flow separation. The variation of C_p over the entire length of the HITPR is shown in Fig. 4.

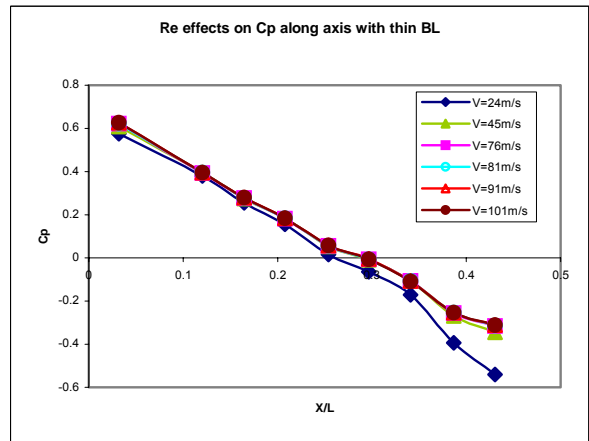


Fig. 3. The variation of C_p along the leading edge of the HITPR in the wind axis.

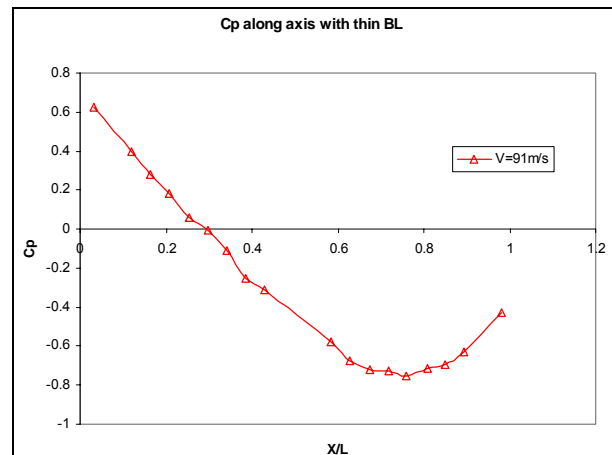


Fig. 4 The variation of C_p in the wind axis over the entire length of the HITPR

1.2 Quad Disk Measurements

Static pressure measurements using the HITPR were compared with those of a quad disk device (Nishiyama and Bedard, 1991). The quad disk static pressure gauge (QDSP), was tested simultaneously with the HITPR at increasing wind speeds until mechanical failure of the QDSP occurred. For wind speeds from 15 m/s to 50 m/s, the error in the quad disk static pressure increased from about 0.2% to 0.6%. At 50 m/s, the small lower disk in the head of the QDSP detached from the central tube. Hence the quad disk showed a high degree of accuracy until failure at 50 m/s.

1.3 Boundary Layer Effects on the Location of C_p

To investigate the influence of the ground boundary layer on C_p , two different boundary layer profiles were generated in the wind tunnel. This was done by using two different leading edges for the ground plane on which the wind tunnel tests were conducted. The velocity profile was measured for a blunt profiled edge and a trip bar. Fig.5 shows that for the blunt profiled edge, the boundary layer thickness was approximately 1.3 cm. For the trip bar, the boundary layer was much thicker at over 15 cm, as shown in Fig. 6.

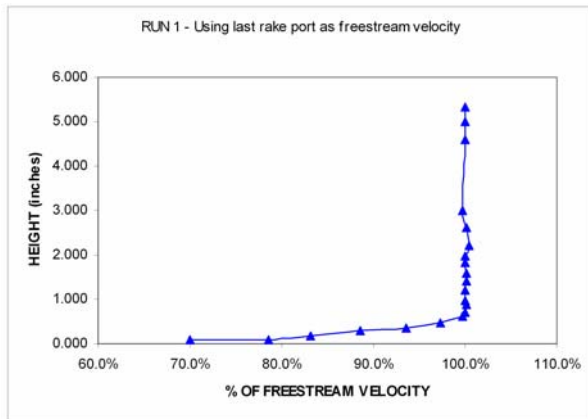


Fig. 5. Velocity profile of the boundary layer with the blunt profiled edge measured at a free-stream velocity of 24 m/s.

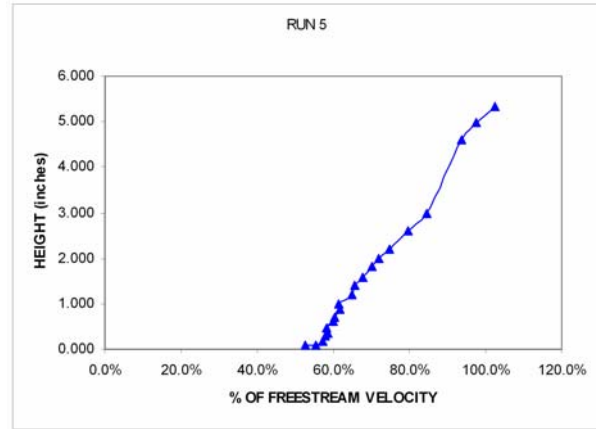


Fig. 6. Velocity profile of the boundary layer with the trip bar measured at a free-stream velocity of 71 m/s.

The main characterization of the C_p variation on the HITPR was performed with a thin boundary layer (Fig 3.). C_p measurements with a thick boundary layer were performed at a wind speed of 76 m/s, and are shown along with the thin boundary layer measurements in Fig. 7. The dependence of C_p with X/L changes markedly for a thicker boundary layer, especially at small values of X/L , i.e. near the front of the model. The effect is smaller however for X/L values over 0.2. Near the $C_p=0$ location, there is a difference of about 0.05 in C_p between the thick and thin boundary layer cases. Since any variations of C_p influences the static pressure measurements of the HITPR, different boundary layers would cause a measurement error. In our present tests however, strong variations in the boundary layer thickness were found to have a relatively small influence on C_p near the $C_p=0$ point.

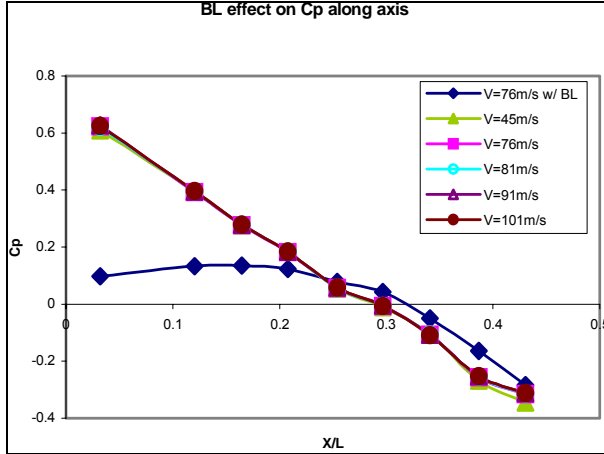


Fig. 7 The variation of C_p in the wind axis for the HITPR in the presence of thin and thick ground boundary layers. The variation of C_p with a thick boundary layer is shown with diamond data points.

1.4 Angular Dependence of C_p for the HITPR

The angular dependence of C_p provided a means of estimating both the wind speed and direction. The variation of C_p at different angles around the HITPR at a radius of 10 cm is shown in Fig. 8. Because C_p is mostly negative in all directions, the radial axis of the plot shows the negative value of C_p . C_p was measured at a single wind speed of 90 m/s, but as indicated in Fig. 3, C_p does not vary with wind speeds above 45 m/s. The pattern shows that for 0 degrees (directly facing the wind), C_p is zero, indicating that the pressure is equal to the free-stream static pressure. As the angle increases, C_p becomes more negative reaching a minimum near 80 degrees. The region of constant C_p on the downstream side of the HITPR is likely caused by the turbulent wake of the cone.

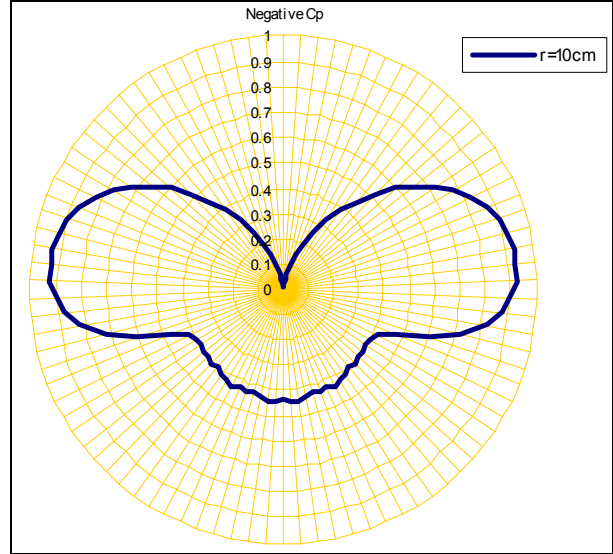


Fig. 8 Angular dependence of negative C_p at a radius of 10 cm and a wind speed of 90 m/s.

Thanks to the strong angular variation of C_p , (Fig. 8) it was possible to establish a method of unambiguously determining the wind direction. By placing a ring of pressure ports at a radius of 10 cm, the angular variation could be measured simultaneously. Since the pressure is highest in the direction facing the wind (Fig. 8), the pressure port with the highest pressure will indicate the direction from which the wind is coming from. The measurement at this point is equal to the free-stream static pressure. Thus, once the wind direction has been determined, the free-stream static pressure is also known.

The wind speed V can be determined by using the measured pressure at a known angle from the wind axis and the expression:

$$V = \sqrt{\frac{2(P_{m\theta} - P_s)}{\rho C_{p\theta}}}$$

Eq. 2. Expression used to infer the wind speed from pressure measurements.

where $P_{m\theta}$ is the measured pressure at a certain angle θ (other than 0 degrees), P_s is the free-stream static pressure, ρ is the air density, and $C_{p\theta}$ is the pressure coefficient at the angle θ . Since the pressure is measured by the HITPR simultaneously at several angles around a ring of pressure ports, the pressure at two different angles can be used to calculate the wind speed using Eq. 2.

The angular dependence of C_p is shown for different radii in Fig 9. For radii larger than 10 cm, a positive value of C_p is observed as indicated by the frontal lobe.

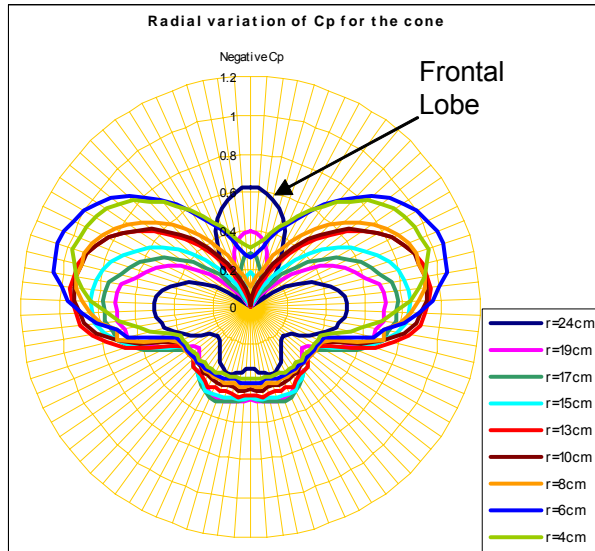


Fig. 9 Angular dependence of C_p on the HITPR at different radii for a wind speed of 90 m/s.

5. FORCE MEASUREMENT ON THE HITPR

The lift, moment, and drag coefficients were measured for the HITPR. The corresponding forces were used to evaluate the likelihood of the HITPR being displaced in high winds. The results are described below:

1.5 Lift Force

The lift forces at different wind speeds were measured for the HITPR are shown in Fig. 10. The horizontal line indicates the downward force due to gravity assuming a HITPR mass of 22.7 kg (50 lbs). The data points labeled “flat top” were obtained for an alternate HITPR shape that was not used in the final design. Forces above the horizontal line should be capable of lifting the HITPR off the ground. These measurements indicate that the HITPR is unlikely to lift off until the wind speed exceeds about 80 m/s.

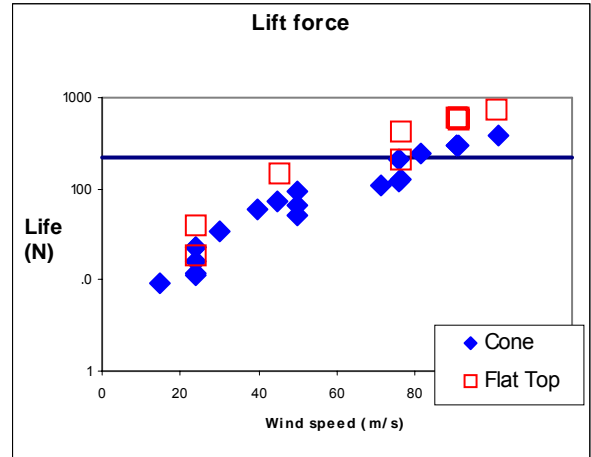


Fig. 10 Lift calculated for the HITPR for different wind speeds. The horizontal line indicates the downward force due to gravity assuming a 22.7 kg (50 lbs) mass for the HITPR.

1.1 Moments

The moment indicates the tendency of the model to rotate vertically, normal to the wind axis, effectively flipping over. The moment was measured for different wind speeds as shown in Fig. 11. Although one may expect that high winds would lift the front edge of the HITPR (facing the wind) causing it to turn upside down, the moment measurements suggest the opposite scenario. Since the pressure is lower at the downstream edge than at the upstream edge (Fig 4), the wind moment in fact induces a rotational force where the front edge of the HITPR is pushed downwards into the ground, and the rear is lifted. This type of moment is favorable to the stability of the HITPR in high winds.

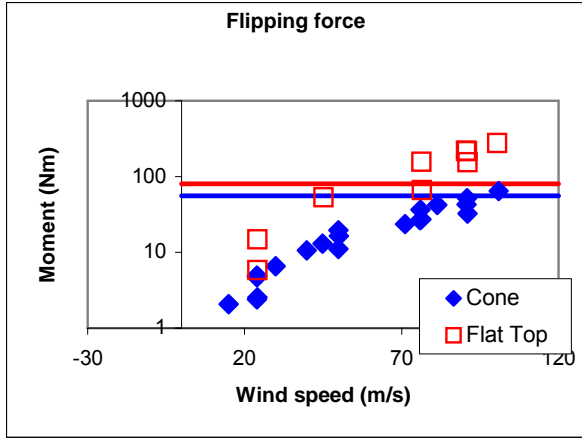


Fig. 11 Moment calculated for the HITPR for different wind speeds. The horizontal line indicates the downward moment due to gravity assuming a 22.7 kg (50 lbs) mass for the HITPR.

1.2 Drag

The drag force indicates the tendency of the HITPR to be pushed along the ground by the wind. The drag force was calculated for different wind speeds and the results are shown in Fig. 12. The stability of the HITPR depends on the friction force between the base of the HITPR and the ground. Consequently, the HITPR should preferably be deployed on rough surfaces.

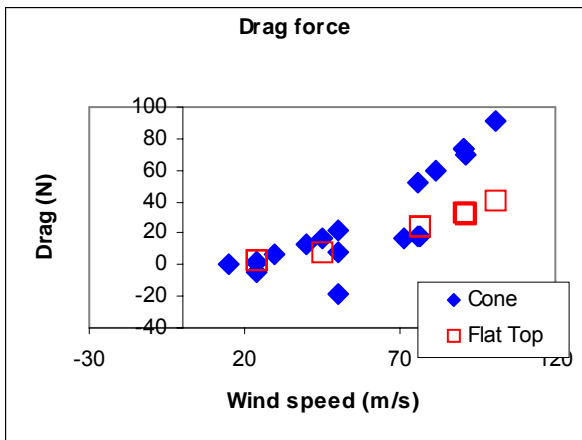


Fig. 12 Drag force calculated for the HITPR for different wind speeds.

6. DATA RESULTS

The results of In-Situ tornado measurements are presented for an F-3 tornado near Pratt, Kansas on May 7th, 2002.

Additional measurements have also been successfully performed using the HITPR on an F-0 tornado near Stratford, Texas on May 15th, 2003, and an F-4 tornado that destroyed the hamlet of Manchester, South Dakota. These results will be presented in future publications.

1.6 F-3 Tornado near Pratt, Kansas on May 7th, 2002

A series of moderate to strong tornadoes touched down within Kiowa and Pratt Counties in Kansas between 2250 and 2000z. ARA deployed one probe on the strongest tornado of the day, an F-3 (Fig. 13), which destroyed several farmhouses. The HITPR probe was located just on the edge of the condensation funnel on the north side. Fig. 14 shows the actual track of the tornado and the probe's position upon passage as well as the position of the HITPR. The tornado was driven by a gust front to the north of the tornado which accounts for the 160 degree movement to the south. The inset picture is the damaged/destroyed farmhouse depicted in the track.



Fig. 13 Video frame grab of large tornado just after it passed near the HITPR probe.



Fig. 14. Tornado track outlined in red, inset picture shows the farmhouse

Fig. 15 shows both the static pressure measured on the HITPR surface at the $C_p = 0$ point and the pressure measured by a pressure port within the HITPR. The static pressure measured at the $C_p = 0$ point is labeled "P-man" and the pressure measured inside the HITPR body was labeled "P-int". Note that both traces are very similar, but that P-int is slightly lower than P-max. This is consistent with previous calibration measurements showing a slightly-offset pressure reading made within the HITPR shell. Although the condensation funnel only passed the HITPR probe on the side, a 24 millibar pressure depression was recorded. This pressure drop is similar to the 26 and 55 mbar pressure drops recorded near a tornado that touched down close to Allison, Texas on June 8th, 1995 (Winn WP et. al. 1999). The Allison tornado also produced damage from F0 to F4 (Rasmussen 1995), which is comparable to the F3 damage produced by the Pratt tornado.

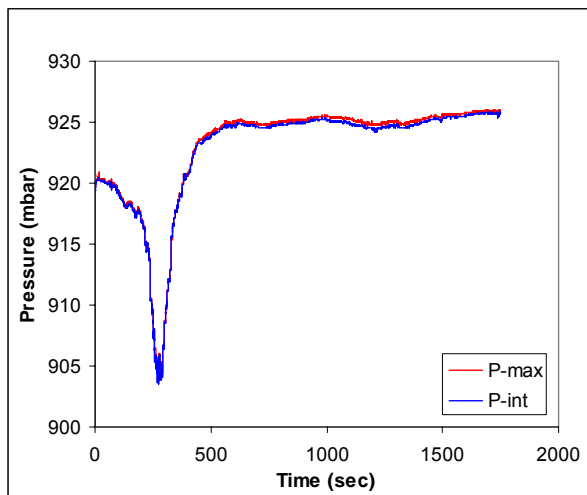


Fig. 15 Pressure trace for the Pratt, Kansas tornado on May 7th, 2002.

Wind speed was also calculated from angular pressure measurements on the HITPR as shown in Fig. 16. A peak of 31 meters/second occurred 300 seconds after deployment. This measurement of wind speed is 76 millimeters about the ground surface and is likely to differ from wind speeds at higher elevations above the ground. The rather chaotic representation of the wind direction is partially due to the smaller angular pressure differences due to lower wind speed as the tornado approached, and moved off. A video camera was also placed near the HITPR (Fig. 14), and approximate wind speeds were inferred objects lofted by the wind moving across

the field of view. These wind speed estimates were in agreement with those measured by the HITPR. The highest wind speeds as observed by the video camera occurred approximately 300 sec after probe deployment, which also agrees with the HITPR measurements.

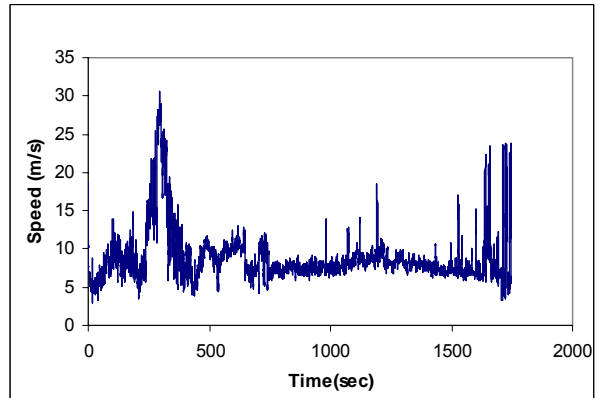


Fig. 16. Wind speed measurements for the Pratt, Kansas tornado on May 7th, 2002.

The wind direction measurements by the HITPR were compared with the direction inferred from the video camera recordings, and were also found to be in rough agreement. These data are shown in Fig. 17 where the HITPR direction measurements are shown in the solid blue line and the inferred direction from the video camera are shown with red triangle points. The HITPR measurements show many rapid fluctuations in the wind direction that may be due to local features in the flow field such as sub-vortices. The global trend of the measurements agree with direction inferred from the video camera.

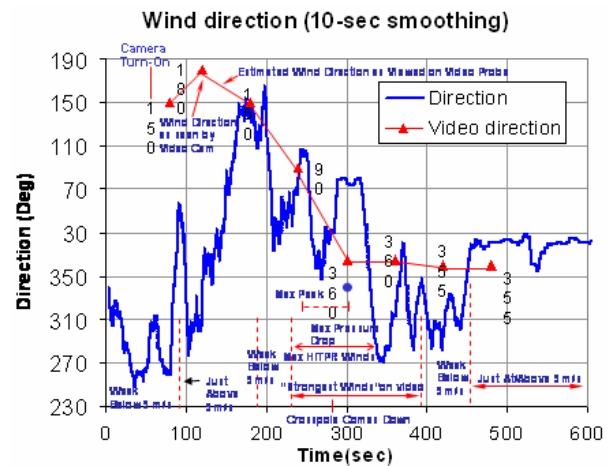


Fig. 17 Wind direction measurements for the Pratt, Kansas tornado on May 7th, 2002.

The temperature of the ambient air was recorded inside the HITPR near the top of the cone (Fig. 18). Temperatures of about 80 degrees were observed at the time of probe deployment. The temperature decreased to approximately 74 degrees upon tornado passage (at about 300 sec) due to the wind-driven rain and some evaporative cooling on the probe surface. The temperature continued to drop after tornado passage due to the passage of the cold front at about 500 seconds. At this point, the sensors were believed to be contaminated by rain water driven into the probe by the wind.

Temperature Data

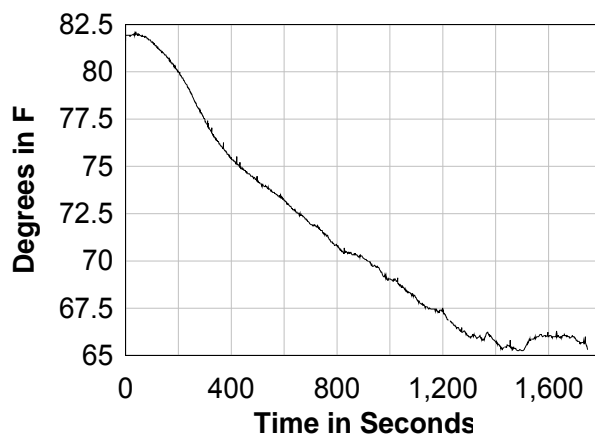


Fig. 18 Temperature measurements for the Pratt, Kansas tornado on May 7th, 2002.

The dewpoint was obtained from relative humidity measurements inside the HITPR (Fig. 19). The sharp rise of the dewpoint temperature from 0 to 100 seconds is mainly due to the abrupt increase of moisture from moving the probe from the vehicle to its placement on the ground. After tornado passage, the air became saturated (100 % relative humidity) at about 500 seconds where it is believed the humidity sensor became contaminated.

Dewpoint Temperature

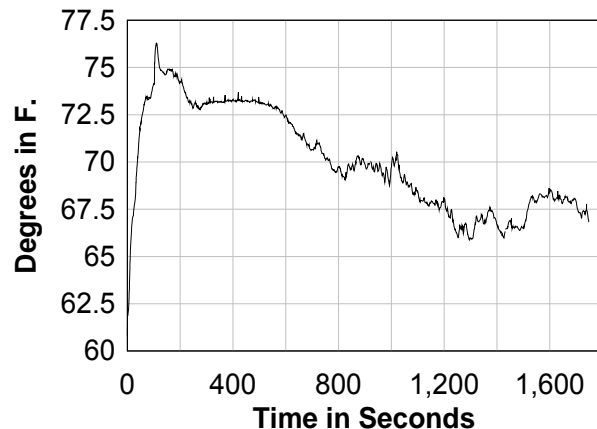


Fig. 19 Dewpoint measurements for the Pratt, Kansas tornado on May 7th, 2002.

7. CONCLUSIONS

A hardened probe called a HITPR was designed and built to measure the free-field static pressure (true barometric pressure), wind speed and direction near the ground, air temperature and relative humidity inside a tornado. The probe has autonomous power and data logging capabilities, as well as a profiled outer shell to minimize aerodynamic wind forces. The pressure measurements are performed thanks to the unique body shape, which features a single radial location where the pressure coefficient is zero, hence providing a unique location where the pressure on the probe surface is equal to the free-field static pressure. The HITPR was completely characterized aerodynamically and calibrated in a wind tunnel at speeds of up to 101 m/s. The location of the $C_p=0$ point on the HITPR was accurately measured and found to be at a non-dimensionalized distance X/L of 0.3 from the front edge of the body. Wind tunnel measurements were used to determine the angular dependence of C_p , which was then used to directly calculate the wind speed from simultaneous angular pressure measurements. Boundary layer effects were investigated and were found to be weak at the $C_p=0$ point. At low wind speeds below 50 m/s, the Reynolds number effects were found to influence C_p .

The calibrated HITPR probe was deployed successfully, nearly in the direct path of an F-3 tornado near Pratt, Kansas, on May 7th, 2002. Measurements were taken of the static pressure, wind speed, wind direction, temperature, and relative humidity. The measurements were found

to be consistent with previous pressure measurements near a similarly large tornado in Allison, Texas. Wind speed and wind direction measurements inferred from a video camera deployed near the probe also confirmed the measurements from the HITPR.

The HITPR hence provides a very robust instrument for accurately measuring the free-field static pressure as well wind speed, wind direction, temperature and relative humidity near the ground in very harsh environments. The operation of the HITPR has been confirmed by a successful deployment near an actual tornado.

8. ACKNOWLEDGEMENT

The authors gratefully acknowledge the support and encouragement of Dr. Joseph Bishop and Dr. Al Bedard. This work is funded by the Department of Commerce/NOAA.

9. REFERENCES

Nishiyama RT and Bedard Jr. AJ. (1991). "A "Quad-Disc" static pressure probe for measurement in adverse atmospheres: with a comparative review of static pressure probe designs", *Rev. Sci. Instrum.* 62 (9). pp. 2193-2204.

Rasmussen EN, Crosbie C, and Kaufman K. (1995). "8 June 1995 Allison tornado damage track", National Severe Storms Laboratory of the National Oceanic and Atmospheric Administration, Norman, OK, <http://doplight.nssl.noaa.gov/projects/vortex/events/damage/allison.html>.

Win WP, Hunyady SJ, and Aulich GD. (1999). "Pressure at the ground in a large tornado", *Journal of Geophysical Research*, Vol. 104, No. D18, pp. 22067-22082.